

# A Weak-Form Combined Source Integral Equation with Explicit Inversion of the Combined-Source Condition

Jonas Kornprobst, *Student Member, IEEE*, and Thomas F. Eibert, *Senior Member, IEEE*

**Abstract**—The combined source integral equation (CSIE) for the electric field on the surface of a perfect electrically conducting scatterer can be discretized very accurately with lowest-order Rao-Wilton-Glisson basis and testing functions if the combined-source (CS) condition is enforced in weak form. We introduce a technique to accelerate the iterative solution for this kind of CSIE. It is demonstrated that the iterative solution of the equation system can be performed very efficiently by explicitly inverting the weak-form CS condition in any evaluation of the forward operator. This reduces the number of unknowns and results in improved convergence behavior at negligible, linear cost. Numerical results demonstrate that the new CSIE outperforms the classical CFIE for high-accuracy simulations.

**Index Terms**—electromagnetic scattering, Rao-Wilton-Glisson functions, combined source integral equation, accuracy, low-order discretization

## I. INTRODUCTION

ELECTROMAGNETIC radiation and scattering problems involving perfect electrically conducting (PEC) objects are often treated by boundary integral equations (IEs) due to their low discretization effort and good accuracy. Common formulations for the tangential field components on the surface of the scatterer are the electric field IE (EFIE) and the magnetic field IE (MFIE) [1]. To obtain a system of equations with one unique solution, i.e. avoiding the interior resonance problem, a combination of the two equations into the combined field IE (CFIE) [2] is the most common solution.

However, a combination of electric and magnetic sources to the combined source IE (CSIE) [3] is also possible; this involves the EFIE and MFIE operators as well and is sometimes known under a different name, the Brackhage-Werner trick [4]–[8]. A related concept (without physical currents) are the single-source surface IEs (SSSIEs), which commonly only employ one type of current unknowns [9]–[15].

With lowest-order div-conforming expansion functions on a triangular mesh, the Rao-Wilton-Glisson (RWG) functions [16], the discretization of the MFIE operator and also of the CFIE, is not accurate [17]. Therefore, the Buffa-Christiansen (BC) functions, which reside in the dual space

of the RWG functions, have been successfully employed as testing functions for an accurate mixed discretization of the MFIE [18]. For the CSIE as well, BC basis functions have been demonstrated to produce accurate results [19]. Rather recently, we demonstrated that an accurate and interior-resonance-free formulation of the CSIE with pure RWG discretization is also possible with an RWG-tested EFIE [20]. Thereby, the tangential electric field  $\mathbf{n} \times \mathbf{n} \times \mathbf{E}$  is tested with RWG functions and the combined source (CS) side condition is also implemented with RWG and  $\mathbf{n} \times \text{RWG}$  functions. Both electric and magnetic equivalent surface current densities are modeled with the div-conforming RWG basis functions, which leads to double the number of unknowns.

In this letter, we employ the CSIE discretization first in a dual-source manner, but reduce it then to a discrete SSSIE: the weak-form CS condition is explicitly solved in an iterative solver, leading to faster iterative solver convergence. In addition, the number of unknowns is reduced by a factor of two. First, we present the formulation and discretization of the CSIE. Next, the discretization and implementation strategy of the CS condition is discussed. Following that, simulation results demonstrate the excellent accuracy and improved iterative solver convergence and conditioning of the novel formulation of the RWG-discretized CSIE.

## II. THE COMBINED SOURCE INTEGRAL EQUATION

### A. Formulation

According to the Huygens principle, a PEC scattering scenario is described by the boundary condition

$$\mathbf{n}(\mathbf{r}) \times \mathbf{E}(\mathbf{r}) = \mathbf{n}(\mathbf{r}) \times \mathbf{E}^{\text{inc}}(\mathbf{r}) + \mathbf{n}(\mathbf{r}) \times \mathbf{E}^{\text{sca}}(\mathbf{r}) = \mathbf{0}, \quad (1)$$

i.e. the superposition of the incident field  $\mathbf{E}^{\text{inc}}$  and the scattered field  $\mathbf{E}^{\text{sca}}$  vanishes on the surface  $S_0$  of the scatterer. The CSIE employs both electric and magnetic surface current densities  $\mathbf{J}_S(\mathbf{r})$  and  $\mathbf{M}_S(\mathbf{r})$  on  $S_0$  as equivalent sources to model the scattered fields. Expressing  $\mathbf{E}^{\text{sca}}$  in terms of the equivalent currents for a suppressed time factor  $e^{j\omega t}$ , the EFIE

$$\begin{aligned} \mathbf{n}(\mathbf{r}) \times \mathbf{E}^{\text{inc}}(\mathbf{r}) = \mathbf{n}(\mathbf{r}) \times \iint_{S_0} \nabla G_0(\mathbf{r}, \mathbf{r}') \times \mathbf{M}_S(\mathbf{r}') \, d\mathbf{s}' \\ + \frac{1}{2} \mathbf{M}_S(\mathbf{r}) + jk_0 Z_0 \mathbf{n}(\mathbf{r}) \times \left[ \frac{1}{k_0^2} \nabla \iint_{S_0} G_0(\mathbf{r}, \mathbf{r}') \nabla' \cdot \mathbf{J}_S(\mathbf{r}') \, d\mathbf{s}' \right. \\ \left. + \iint_{S_0} G_0(\mathbf{r}, \mathbf{r}') \mathbf{J}_S(\mathbf{r}') \, d\mathbf{s}' \right] \quad (2) \end{aligned}$$

Manuscript received February 2, 2018; revised August 29, 2018; accepted August 29, 2018; date of this version August 29, 2018. (Corresponding author: Jonas Kornprobst.)

The authors are with the Chair of High-Frequency Engineering, Department of Electrical and Computer Engineering, Technical University of Munich, 80290 Munich, Germany (e-mail: j.kornprobst@tum.de).

Color versions of one or more of the figures in this letter are available online at <http://ieeexplore.ieee.org>.

Digital Object Identifier 10.1109/LAWP.2018.2869926

is a more detailed version of (1). The involved scalar Green's function of free space is

$$G_0(\mathbf{r}, \mathbf{r}') = \frac{e^{-jk_0|\mathbf{r}-\mathbf{r}'|}}{4\pi|\mathbf{r}-\mathbf{r}'|} \quad (3)$$

with source coordinate  $\mathbf{r}'$  and observation coordinate  $\mathbf{r}$ , the free-space wave number  $k_0$  and the free-space wave impedance  $Z_0$ . Since the equivalent sources are not the Love currents, and thus ambiguous, the CS constraint

$$\mathbf{M}_S(\mathbf{r}) = \alpha Z_0 \mathbf{n}(\mathbf{r}) \times \mathbf{J}_S(\mathbf{r}) \quad (4)$$

can be enforced to obtain a unique combination of electric and magnetic surface current densities, i.e. a quadratic system of equations with the same number of unknowns as equations. The combination parameter  $\alpha$  is typically chosen as unity to achieve balanced contributions of electric and magnetic currents to the radiated fields [3].

### B. Discretization

The discretization of (2) with RWG functions  $\beta_n$ , defined on the  $n$ th pair of neighboring triangles, is well-known. Suitable testing functions in the dual space of the electric field  $\mathbf{n} \times \mathbf{n} \times \mathbf{E}$  are  $\beta$  functions. The MoM equation system for PEC objects is written as

$$\left[ -\frac{1}{2}\mathbf{A} + \mathbf{K} \right] \mathbf{v} + jk_0 Z_0 \mathbf{T} \mathbf{i} = \mathbf{e} \quad (5)$$

with the matrix elements of  $\mathbf{K}$  and  $\mathbf{T}$  defined in [21] and the currents discretized as a summation of RWG basis functions

$$\mathbf{J}_S = \sum_{n=1}^N \beta_n i_n, \quad \mathbf{M}_S = \sum_{n=1}^N \beta_n v_n. \quad (6)$$

Furthermore, we discretize the combined source condition (4) in the same way, by expanding the currents according to (6) and testing the equation with RWG functions. This gives the additional equation system

$$\mathbf{A}' \mathbf{v} - \alpha Z_0 \mathbf{A} \mathbf{i} = \mathbf{0}, \quad (7)$$

where the Gram matrix  $\mathbf{A}$  linking  $\beta$  and  $\mathbf{n} \times \beta$  functions has the entries

$$A_{mn} = \iint_{S_m} \beta_m(\mathbf{r}) \cdot (\mathbf{n} \times \beta_n(\mathbf{r})) \, ds \quad (8)$$

and the Gram matrix  $\mathbf{A}'$  of the RWG functions is defined with the entries

$$A'_{mn} = \iint_{S_m} \beta_m(\mathbf{r}) \cdot \beta_n(\mathbf{r}) \, ds. \quad (9)$$

Overall, we obtain the complete CSIE equation system

$$\begin{bmatrix} jk_0 Z_0 \mathbf{T} & -\frac{1}{2}\mathbf{A} + \mathbf{K} \\ -\alpha Z_0 \mathbf{A} & \mathbf{A}' \end{bmatrix} \begin{bmatrix} \mathbf{i} \\ \mathbf{v} \end{bmatrix} = \begin{bmatrix} \mathbf{e} \\ \mathbf{0} \end{bmatrix}. \quad (10)$$

Since (10) has electric and magnetic current unknowns, it is referred to as CSIE-JM in the following. In this formulation, as it has been presented in our previous work [20], the discretized weak-form CS condition (7) augments the EFIE as a side condition. As it will be demonstrated by numerical simulations, this formulation has conditioning disadvantages compared to a formulation with only one of the sources as unknowns. It is important to note that the conditioning of (10)

is improved considerably if the magnetic current unknowns are replaced by the weighted version

$$\mathbf{v}' = \mathbf{v}/Z_0 \quad (11)$$

and the correct magnetic current coefficients are retrieved in the end by a multiplication with  $Z_0$ . Alternatively, a diagonal preconditioner shows similar benefits.

To improve the implementation of the CSIE, the Gram matrices are stored separately and only the symmetric matrices  $\mathbf{K}$  and  $\mathbf{T}$  remain to be stored for the system matrix. The memory consumption of the Gram matrices is negligible with linear complexity, since  $\mathbf{A}$  contains  $4N$  and  $\mathbf{A}'$   $5N$  real-valued entries. To reduce the number of unknowns, and halve the memory consumption of the iterative solver of the whole system, which is a generalized minimum residual (GMRES) solver, the side condition (7) is solved explicitly within each matrix vector product according to

$$\mathbf{v} = \alpha Z_0 \mathbf{A}'^{-1} \mathbf{A} \mathbf{i}, \quad (12)$$

where  $\mathbf{A}'^{-1}$  denotes the inverse of  $\mathbf{A}'$  which is also obtained in an iterative manner by using the conjugate gradient method. The Gram matrix  $\mathbf{A}'$  is well-conditioned and the solver (with diagonal preconditioning) needs only a few iterations for a low residual error. Due to the linear matrix size, the convergence time of this inner iterative solver is negligible. We obtain the CSIE with electric current unknowns only (CSIE-J)

$$\left[ \alpha Z_0 \left( -\frac{1}{2}\mathbf{A} + \mathbf{K} \right) \mathbf{A}'^{-1} \mathbf{A} + jk_0 Z_0 \mathbf{T} \right] \mathbf{i} = \mathbf{e}. \quad (13)$$

The magnetic currents are calculated in a post-processing step according to (12) since it is not necessary to store them during the solution process.

In general, the easiest way to accelerate the iterative solver convergence is diagonal preconditioning. For the CSIE-J, we investigate two possibilities. One possibility is to neglect the influence of the magnetic currents on the main diagonal and use only the diagonal matrix

$$\mathbf{D} = jk_0 Z_0 \text{diag}(\mathbf{T}) \quad (14)$$

for the preconditioning of (13). Since the inverse of  $\mathbf{A}'$  is not directly available, only the main diagonal is taken to estimate the inverse. Hence, the matrix

$$\mathbf{D} = jk_0 Z_0 \text{diag}(\mathbf{T}) - \alpha Z_0 \text{diag}(\mathbf{A} \text{diag}(\text{diag}(\mathbf{A}'))^{-1} \mathbf{A}) \quad (15)$$

can alternatively be employed for preconditioning.

### III. NUMERICAL RESULTS

For evaluating the performance of the two forms of the CSIE, they are compared to the accurate but ill-conditioned EFIE and to the well-conditioned but inaccurate MFIE. The common CFIE with combination parameter 0.5 is also considered, which is comparable to  $\alpha = 1$  in the CSIE.

First, the convergence behavior with mesh refinement is analyzed for a 1 m square cube with plane wave illumination with a wavelength of 2 m. To analyze the MFIE operator within the CSIE on its own, a combination parameter  $\alpha = 10$  is chosen for the mesh refinement analysis. We consider three

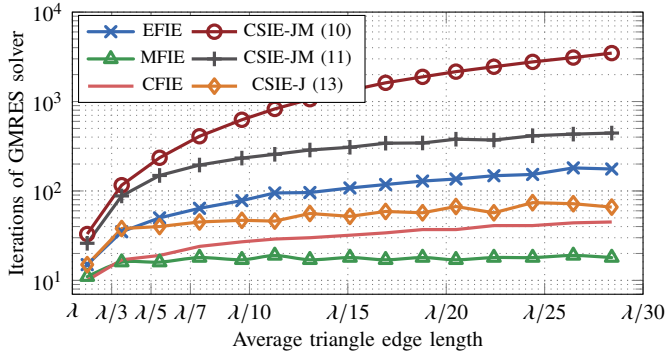


Figure 1. Iterative solver convergence analysis for the mesh refinement of a 1 m square cube.

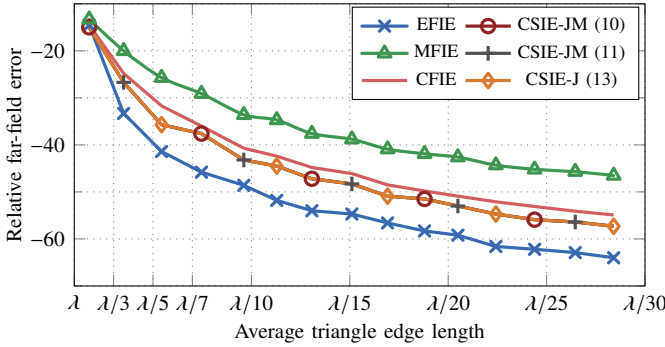


Figure 2. Scattered far-field accuracy for the 1 m square cube.

different formulations of the CSIE: first the straight-forward version CSIE-JM (10) as originally proposed in [20], then the modified CSIE-JM with weighted magnetic currents according to (11), and finally the novel formulation (13). In Fig. 1, the iterative solver convergence behavior to a residual error of  $10^{-4}$  is analyzed. The new CSIE-J formulation shows an acceptable convergence, faster than the EFIE and almost as fast as the CFIE. For this small example, in the absence of interior resonances, the CSIE-JM is much slower than the EFIE and, thus, the formulation with the slowest iterative solver convergence in this comparison. The block-diagonal preconditioning can only overcome this in part. In Fig. 2, the averaged error of the scattered far-field with respect to a higher-order EFIE solution on the finest mesh is shown. As expected, both CSIE-J and CSIE-JM show almost exactly the same error level, which is about 10 dB better than the error of the MFIE. The EFIE solution is even about 5 dB more accurate. The performance difference of CFIE and CSIE-J will be analyzed in the following more carefully in order to highlight the benefits of the novel CSIE-J. It will be shown that only this CSIE is able to outperform the CFIE.

A PEC sphere with a diameter of 1 m and 999 electric current unknowns is considered. In the simulated frequency range, the average edge length of the mesh is between  $\lambda/25$  and  $\lambda/7$ . The first two interior resonances, corresponding to the resonance frequencies of a spherical PEC cavity with the same diameter, are observed for the EFIE and the MFIE. In Fig. 3, the iterative solver convergence of a GMRES solver is analyzed for a residual error of  $10^{-4}$ . In the CSIE-J, the

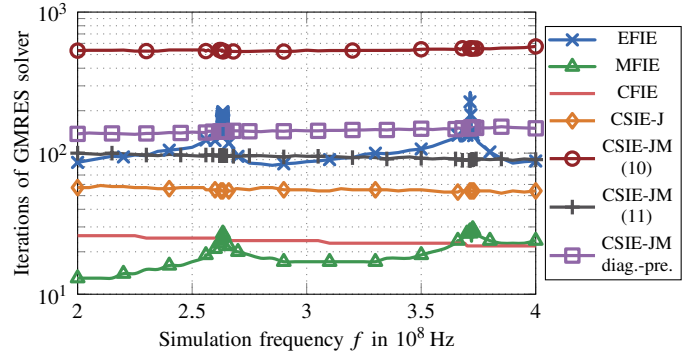


Figure 3. Iterative solver convergence analysis for the first two resonances of a PEC sphere with a diameter of 1 m.

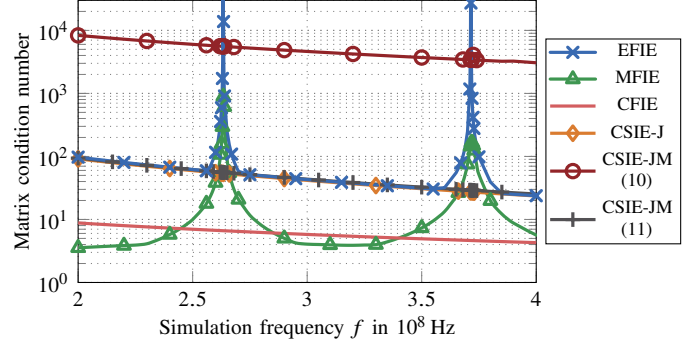


Figure 4. Condition number around the first two resonances of a 1 m sphere.

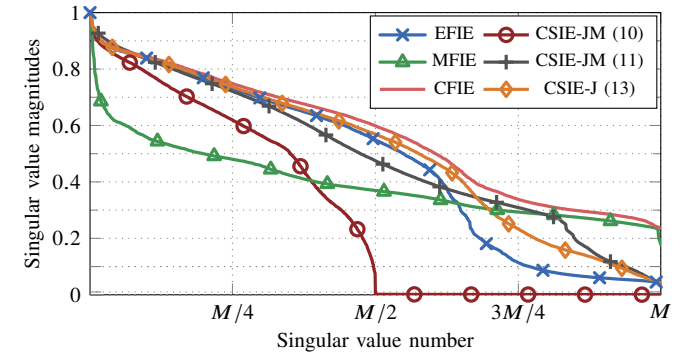


Figure 5. Normalized singular value spectra for the PEC sphere at 0.4 GHz. For  $J$  and  $M$  unknowns,  $M = 1998$ , else  $M = 999$ .

inversion of the Gram matrix for the side condition is solved to a residual error of  $10^{-5}$ , which is one order of magnitude lower. The EFIE, MFIE, CFIE and CSIE-J solutions are obtained without preconditioning; the CSIE-JM (10) is solved without preconditioning, with diagonal preconditioning and with block-diagonal preconditioning according to (11). Both EFIE and MFIE suffer from the interior resonances due to a null space at resonance frequencies. The CFIE and both CSIE formulations show a stable convergence behavior, while only CSIE-J is faster than the EFIE on average. In addition, the matrix condition numbers without preconditioning (except for CSIE-JM) are shown in Fig. 4. Again, the CFIE and CSIE formulations have the advantage of an absolutely stable condition number at interior resonance frequencies. However, one observation is remarkable: While the EFIE, CSIE-J and

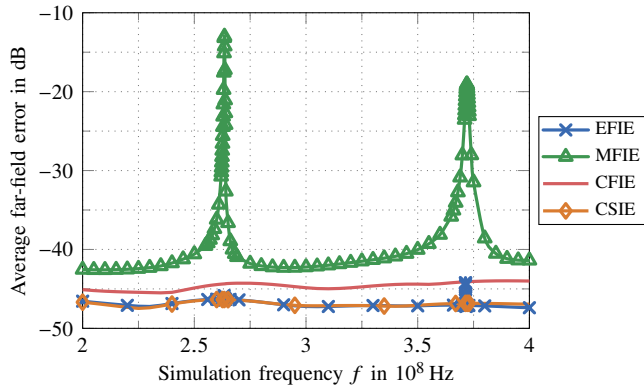


Figure 6. Accuracy analysis around the first two resonances of a PEC sphere.

both preconditioned CSIE-JM equations show almost the same condition number, the iterative solver convergence of the CSIE-J is much better. The most reasonable cause is a different eigenvalue distribution in the complex plane, e.g. by an improved clustering more suitable for GMRES. In the singular-value spectrum, see Fig. 5, we can recognize a certain amount of singular values with larger values for the CSIE-J as compared to the EFIE. The better iterative solver convergence of CSIE-J has been verified for many different right-hand sides, including random vectors and unit vectors of the standard basis. Furthermore, the accuracy as compared to the analytical Mie series solution is shown in Fig. 6. It is observed that the MFIE shows the poorest accuracy, with huge deteriorations at the resonance frequencies. Compared to this behavior, the EFIE only shows inaccuracies quite exactly at the resonance frequencies. The CFIE is influenced by the MFIE error and, thus, its accuracy is worse than the CSIE. Both CSIE formulations show absolutely the same error level, as expected, which is also about the same as the EFIE error.

As a further problem, the stealth object Flamme is simulated with  $\lambda/10$  mean edge length discretization and 287 922 electric current unknowns [22], [23]. The MFIE takes 1267 iterations for convergence to a residual error of  $10^{-5}$ , the CFIE 315, the CSIE-J 448, and the CSIE-JM 1264 iterations. The EFIE did not converge without preconditioning even after thousands of iterations. With diagonal preconditioning, the iterative solution of the MFIE is accelerated to 899 iterations and the iterative solution of the CFIE to 253. The CSIE-J converges within 384 iterations if only the EFIE operator is taken for preconditioning and within 381 iterations if the approximated diagonal according to (15) is utilized. The average time per matrix-vector product is 10.5 seconds for EFIE, MFIE, and CFIE, and 20.7 seconds for the CSIE-JM, where all computations have been performed single-threaded on an Intel E5-1650 v4 processor with 3.6 GHz clock speed. The explicit inversion of the CS condition takes only additional 0.04 seconds on average, or about 10 iterations, for a residual error of  $5 \cdot 10^{-7}$ . Results of the bistatic radar cross section are shown in Fig. 7. Compared to an 3rd order EFIE solution on a refined mesh [21], the MFIE shows a maximum error of  $-37.3$  dB, the CFIE of  $-44.2$  dB, both CSIE-J and CSIE-JM of  $-57.8$  dB, and the EFIE of  $59.8$  dB.

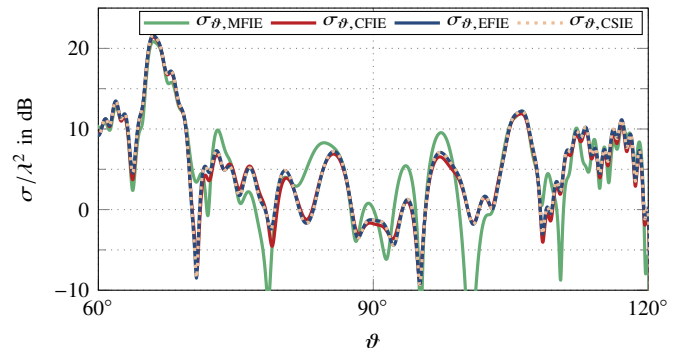


Figure 7. Side-lobe section of the bistatic radar cross section  $\sigma$  of the Flamme for the EFIE, CFIE, and CSIE solutions.

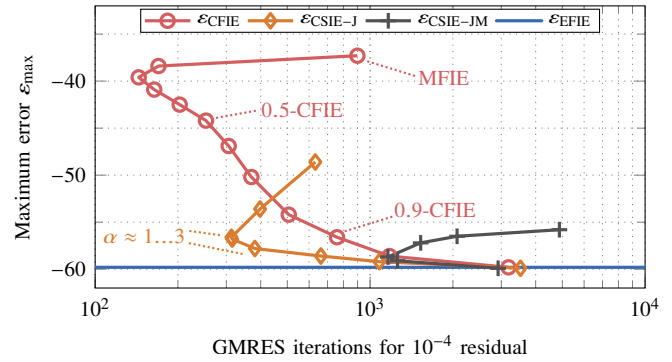


Figure 8. Error level vs. iterations with different weightings in CFIE and CSIE for Flamme.

With a difference in the iterative solver convergence, it is still not clear whether the CSIE-J or the CFIE offer the better accuracy-convergence trade-off. Therefore, we analyze the influence of the corresponding weighting or combination factors for the cases of CSIE-J and CFIE with diagonal preconditioning and CSIE-JM with block-diagonal preconditioning in Fig. 8. The simulated object is again the Flamme with the same parameters as before. It becomes clear that the CSIE-JM can provide the same error level only at the cost of more solver iterations. Additionally, the CSIE-J is able to outperform the CFIE for near-EFIE accuracies. For instance, the CSIE-J with  $\alpha = 2.7$  converges within 313 iterations and offers an error level of 56.6 dB, while the CFIE with combination parameter 0.9 (90% EFIE) converges in 758 iterations for the same error. This still means less than half the solver memory consumption for the CSIE-J, approximately the same memory for the matrices, and about twice the time per matrix-vector-product (but less solution time overall).

#### IV. CONCLUSION

A new form of the CSIE with weak-form CS condition has been introduced, showing an improved iterative solver convergence and a reduced number of unknowns. The magnetic current unknowns are explicitly computed from the electric currents for each matrix-vector product within the iterative solver and, therefore, eliminated. The new CSIE is able to offer a better accuracy/convergence trade-off than the CFIE and the weighting factor in the CSIE is not a critical choice (other than in the CFIE) in order to achieve almost EFIE accuracy.

## REFERENCES

- [1] R. F. Harrington, "Boundary integral formulations for homogeneous material bodies," *J. Electromagn. Waves Appl.*, vol. 3, no. 1, pp. 1–15, Jan. 1989.
- [2] J. R. Mautz and R. F. Harrington, "H-field, E-field, and combined-field solutions for conducting bodies of revolution," *A.E.Ü. (Germany)*, vol. 32, no. 4, pp. 157–164, Apr. 1978.
- [3] J. Mautz and R. Harrington, "A combined-source solution for radiation and scattering from a perfectly conducting body," *IEEE Trans. Antennas Propag.*, vol. 27, no. 4, pp. 445–454, Jul. 1979.
- [4] H. Brakhage and P. Werner, "Über das dirichletsche Außenraumproblem für die Helmholtzsche Schwingungsgleichung," *Archiv der Mathematik*, vol. 16, no. 1, pp. 325–329, 1965.
- [5] A. Buffa and R. Hiptmair, "Regularized combined field integral equations," *Numerische Mathematik*, vol. 100, no. 1, pp. 1–19, 2005.
- [6] M. Darbas, "Generalized combined field integral equations for the iterative solution of the three-dimensional Maxwell equations," *Appl. Math. Lett.*, vol. 19, no. 8, pp. 834–839, 2006.
- [7] O. Steinbach and M. Windisch, "Modified combined field integral equations for electromagnetic scattering," *SIAM J. Numer. Anal.*, vol. 47, no. 2, pp. 1149–1167, 2009.
- [8] J. M. Melenk, "Mapping properties of combined field Helmholtz boundary integral operators," *SIAM J. Math. Anal.*, vol. 44, no. 4, pp. 2599–2636, 2012.
- [9] E. Marx, "Single integral equation for wave scattering," *J. Math. Phys.*, vol. 23, no. 6, pp. 1057–1065, Jun. 1982.
- [10] A. Glisson, "An integral equation for electromagnetic scattering from homogeneous dielectric bodies," *IEEE Trans. Antennas Propag.*, vol. 32, no. 2, pp. 173–175, Feb. 1984.
- [11] M. S. Yeung, "Single integral equation for electromagnetic scattering by three-dimensional homogeneous dielectric objects," *IEEE Trans. Antennas Propag.*, vol. 47, no. 10, pp. 1615–1622, Oct. 1999.
- [12] A. Menshov and V. Okhmatovski, "New single-source surface integral equations for scattering on penetrable cylinders and current flow modeling in 2-D conductors," *IEEE Trans. Microw. Theory Techn.*, vol. 61, no. 1, pp. 341–350, Jan. 2013.
- [13] Y. Shi and C. Liang, "An efficient single-source integral equation solution to EM scattering from a coated conductor," *IEEE Antennas Wireless Propag. Lett.*, vol. 14, pp. 547–550, 2015.
- [14] U. R. Patel, P. Triverio, and S. V. Hum, "A novel single-source surface integral method to compute scattering from dielectric objects," *IEEE Antennas Wireless Propag. Lett.*, vol. 16, pp. 1715–1718, 2017.
- [15] F. S. H. Lori, A. Menshov, R. Gholami, J. B. Mojolagbe, and V. I. Okhmatovski, "Novel single-source surface integral equation for scattering problems by 3-D dielectric objects," *IEEE Trans. Antennas Propag.*, vol. 66, no. 2, pp. 797–807, Feb. 2018.
- [16] S. M. Rao and D. R. Wilton, "E-field, H-field, and combined field solution for arbitrarily shaped three-dimensional dielectric bodies," *Electromagn.*, vol. 10, no. 4, pp. 407–421, Oct. 1990.
- [17] Ö. Ergül and L. Gürel, "Investigation of the inaccuracy of the MFIE discretized with the RWG basis functions," in *Proc. IEEE Antennas Propag. Soc. Symp. (APSURSI)*, Monterey, CA, Jun. 2004, pp. 3393–3396.
- [18] K. Cools, F. P. Andriulli, D. De Zutter, and E. Michielssen, "Accurate and conforming mixed discretization of the MFIE," *IEEE Antennas Wireless Propag. Lett.*, vol. 10, pp. 528–531, 2011.
- [19] P. Ylä-Oijala, S. P. Kiminki, K. Cools, F. P. Andriulli, and S. Järvenpää, "Stable discretization of combined source integral equation for scattering by dielectric objects," *IEEE Trans. Antennas Propag.*, vol. 60, no. 5, pp. 2575–2578, May 2012.
- [20] J. Kornprobst and T. J. Eibert, "A combined source integral equation with weak form combined source condition," *IEEE Trans. Antennas Propag.*, vol. 66, no. 4, pp. 1251–1255, Apr. 2018.
- [21] Ismatullah and T. F. Eibert, "Surface integral equation solutions by hierarchical vector basis functions and spherical harmonics based multilevel fast multipole method," *IEEE Trans. Antennas Propag.*, vol. 57, no. 7, pp. 2084–2093, Jul. 2009.
- [22] L. Gürel, H. Bağcı, J. C. Castelli, A. Cheraly, and F. Tardivel, "Validation through comparison: Measurement and calculation of the bistatic radar cross section of a stealth target," *Radio Sci.*, vol. 38, no. 3, Jun. 2003.
- [23] T. F. Eibert, "A diagonalized multilevel fast multipole method with spherical harmonics expansion of the k-space integrals," *IEEE Trans. Antennas Propag.*, vol. 53, no. 2, pp. 814–817, Feb. 2005.